Journal of Plant Physiology 268 (2022) 153577

Contents lists available at ScienceDirect

Journal of Plant Physiology

journal homepage: www.elsevier.com/locate/jplph

Post-silking ^{15}N labelling reveals an enhanced nitrogen allocation to leaves in modern maize (*Zea mays*) genotypes

Javier A. Fernandez [a,*], Jesse B. Nippert [b], P.V. Vara Prasad [a], Carlos D. Messina [c], Ignacio A. Ciampitti [a,**]

[a] Department of Agronomy, Kansas State University, Manhattan, KS, 66506, United States
[b] Division of Biology, Kansas State University, Manhattan, KS, 66506, United States
[c] Corteva Agriscience, Johnson, IA, 50131, United States

ARTICLE INFO

Keywords:
Allocation
Maize
^{15}N labelling
Nitrogen
Remobilization
Uptake

ABSTRACT

Nitrogen (N) metabolism is a major research target for increasing productivity in crop plants. In maize (*Zea mays* L.), yield gain over the last few decades has been associated with increased N absorption and utilization efficiency (i.e. grain biomass per unit of N absorbed). However, a dynamical framework is still needed to unravel the role of internal processes such as uptake, allocation, and translocation of N in these adaptations. This study aimed to 1) characterize how genetic enhancement in N efficiency conceals changes in allocation and translocation of N, and 2) quantify internal fluxes behind grain N sources in two historical genotypes under high and low N supply. The genotypes 3394 and P1197, landmark hybrids representing key eras of genetic improvement (1990s and 2010s), were grown under high and low N supply in a two-year field study. Using stable isotope ^{15}N labelling, post-silking nitrogen fluxes were modeled through Bayesian estimation by considering the external N (exogenous-N) and the pre-existing N (endogenous-N) supply across plant organs. Regardless of N availability, P1197 exhibited greater exogenous-N accumulated in leaves and cob-husks. This response was translated to a larger amount of N mobilized to grains (as endogenous-N) during grain-filling in this genotype. Furthermore, the enhanced N supply to leaves in P1197 was associated with increased post-silking carbon accumulation. The overall findings suggest that increased N utilization efficiency over time in maize genotypes was associated with an increased allocation of N to leaves and subsequent translocation to the grains.

1. Introduction

Nitrogen (N) is an essential nutrient required for plant growth and development. Nitrogen is absorbed by plants – as nitrate, ammonium, or other organic N forms – and incorporated into numerous metabolites such as amino acids and proteins (Tegeder and Masclaux-Daubresse, 2018). In crop species, much effort has gone into identifying strategies for improving the efficiency on which plants absorb and utilize N for plant growth and development (Sinclair and Rufty, 2015). In cereals, grain production largely depends, along with carbon (C), on the supply of N to sink tissues throughout the plant growth cycle (Ladha et al., 2016). The set of morpho-physiological mechanisms involved in the plant response to N availability during grain development in cereal crop species are of interest to plant breeders seeking to improve yields per unit of N fertilizer applied in crop production.

In maize (*Zea mays* L.), genetic yield improvement over the last few decades has been associated with increased N absorption, complemented by an enhanced crop N utilization efficiency (i.e. grain biomass produced per unit of N absorbed) (Ciampitti and Vyn, 2012; DeBruin et al., 2017; Haegele et al., 2013; Mueller et al., 2019). To further understand the determinants of N changes in plant tissues, a dynamical N framework is needed to unravel the role of the interaction of processes such as N uptake, allocation among organs based on supply and demand signals, and translocation of N during crop growth. Particular interests have been addressed to study N utilization during reproductive stages of crop development where quality, size and yield of seeds is determined in annual crops (Dreccer et al., 2000; Kinugasa et al., 2012; Rossato et al., 2001; Salon et al., 2001; Weiland and Ta, 1992). In

Abbreviations: N, nitrogen; C, carbon; ZN, zero N; FN, full N; SLN, specific leaf N.

* Corresponding author.
** Corresponding author.
E-mail addresses: jafernandez@ksu.edu (J.A. Fernandez), ciampitti@ksu.edu (I.A. Ciampitti).

https://doi.org/10.1016/j.jplph.2021.153577
Received 10 March 2021; Received in revised form 20 November 2021; Accepted 21 November 2021
Available online 26 November 2021

maize, the initiation of this reproductive period is manifested by the release of pollen by the anthers (anthesis) and the emergence of receptive stigmas (silking), indicating male and female floral maturity for pollination. This is recognized as a central phase in N dynamics because uptake and assimilation starts to decline during the post-silking period (Fernandez et al., 2020; Russelle et al., 1983). In addition, recycling of nutrients during senescence allows reutilization of N contained in vegetative organs (e.g. stems and mature leaves) and or translocation to reproductive organs (e.g. developing seeds) after hydrolysis of proteins to amino acids (Lambers et al., 2008). It is known that the plant N balance resulting from the interaction of these processes has been altered over time together with improvements in kernel set (i.e. number of grains per area) of modern genotypes (Ciampitti and Vyn, 2012; Duvick, 2005). However, the complexity of the system has not been fully assessed by studying both the assimilation of external N supply and the remobilization of pre-existing N across organs. Such understanding will enable, for instance, quantifying the impact of breeding on the newly synthesized amino acids that are allocated to the stover before the onset of the leaf N remobilization process (Ta and Weiland, 1992).

Variations in the leaf N dynamics during grain-filling received recent attention as physiological adaptations to modern agriculture (Chen et al., 2015; Kosgey et al., 2013). Because photosynthetic rate is dependent, among other factors, on the leaf N content per unit leaf area (Sinclair and Horie, 1989), improvement in seasonal photosynthesis may arise as a consequence of a superior leaf N status per unit area (Borrell and Hammer, 2000; Vos et al., 2005). It is conceivable that plants with proportionally more N allocated to the leaves at the expense of other organs can maintain photosynthesis rates during grain fill and, therefore, promote biomass production (Hirose and Werger, 1987; Hollinger, 1996). A recent comparison between historical hybrids led to the hypothesis that a longer retention of N in the leaves may underpin an accelerated N translocation from stems at early phases of grain-filling, thus enhancing N utilization efficiency (Fernandez et al., 2021). However, the lack of field-level quantification of the underlying internal N fluxes remains to be determined to further test the above hypothesis.

Due to the relevancy of N economy for maize yield improvement, increased focus to develop models that identify N allocation and transport processes are of the highest priority. From the perspective of crop growth models, a necessary requirement to parametrize the mechanics behind N accumulation is to provide a realistic and efficient method to discriminate or differentiate the recently incorporated N from the pre-existing pool in a plant organ at a given time. The use of N stable isotopic ratios (^{15}N) has been largely demonstrated as an efficient tool to quantify current N absorption and allocation in plants (Knowles and Blackburn, 1993; Yoneyama et al., 2003). In particular for relative N allocation, short-term labelling has been widely employed in hydroponics (Arkoun et al., 2012; Friedrich and Schrader, 1979; Tanemura et al., 2008), or either under controlled environments in growth chambers (Lehmeier et al., 2013; Schiltz et al., 2005) or greenhouses (Avice et al., 1996; Cliquet et al., 1990; Yang et al., 2016). At a field-scale in maize, the use of this technique has been restricted to fewer studies (de Oliveira Silva et al., 2017; Ta and Weiland, 1992). In this study, measures of post-silking N allocation from multiple short-term ^{15}N labelling were assembled using dynamical models. Evidence of N distribution can be incorporated in a framework considering a two-way flux of N across aerial plant organs; thus, enabling the phenotyping of the internal N fluxes in the crop (Crawford et al., 1982; Gallais et al., 2006; Malagoli et al., 2005; Schiltz et al., 2005). Each day, absorbed N is allocated to leaves, stem, cob-husks, and grains (hereafter referred as exogenous-N). Simultaneously, a fraction of the pre-existing N stored in organs (hereafter referred as endogenous-N) is translocated to sink tissues. In this framework, the net N accumulation of an organ is captured as the resulting balance of inward and outward fluxes. With a functional linkage with biomass and yield generation processes, a better understanding of such physiological aspects may help in the identification of promising targets for sustaining future genetic improvement. Furthermore, a biological N dynamics model structured upon such framework could provide the capacity to evaluate the potential value of breeding efforts in plant N utilization traits.

The present study provides an analysis of how the post-silking N allocation and translocation processes have been modified in two genotypes representing eras of genetic improvement (1990s and 2010s) under high and low N supply. By using a dynamical N model considering the external (exogenous-N) and the pre-existing (endogenous-N) N supply in the plant, this study aimed to 1) understand how patterns of allocation and translocation of N underpin genetic enhancement for N efficiency, and 2) quantify internal N fluxes as determinants of grain N.

2. Materials and methods

2.1. Field experiments and phenotypic determinations

A two-year field study was conducted during 2017 and 2018 growing seasons at the Ashland Bottoms Research Farm near Manhattan, KS, US (39°08′ N, 96°37’ W). The experimental sites during 2017 are described in-depth in Fernandez et al. (2021). The analysis in this study includes an additional experimental trial in 2018 with similar agronomic management and design of Fernandez et al. (2021). A detailed description of sites is shown in Table 1. Briefly, the experiments consisted of two irrigated (2017 and 2018) and one rainfed (2017) treatments modeled as a split plot design with two treatment factors and three replicates. Factors evaluated consisted of two maize Pioneer (Corteva Agriscience, Johnston, IA, US) single cross hybrids with different year of release (3394 in 1991; and P1197 in 2014) as main plots, and two N scenarios (zero N, and full N, 137 kg ha^{-1} for the non-irrigated and 218 kg ha^{-1} for the irrigated sites) as subplots. Fertilizer N rates to achieve a high N supply condition (i.e. full N) were adjusted for N demand based on yield target, and plant density based on regional agronomy recommendations for each condition. Size of each plot was 64 m^2 (4 rows at 0.76 cm between rows × 21 m length). Soil analyses were conducted at pre-planting to characterize initial conditions (Table 1). All trials were controlled and conducted free of weeds, pests, and diseases during the growing season.

Key developmental stages (Ritchie et al., 1997), anthesis (VT) and silking (R1) dates were recorded daily for 20 tagged plants per plot, and silking date for the plot was considered when 50% of the plants had exposed silks. For determination of physiological maturity (R6) dates, one ear of a previously tagged plant was collected every 3–4 days per plot, from kernel blister stage (R2) until harvest maturity. Ten kernels from the central portion of the ear were marked and sampled to track changes in kernel dry weight during the entire period. A bilinear model was fitted to the data of each experimental unit (N treatment x genotype x replicate x site) with the form:

$$Grain\ weight\ \left(mg\ grain^{-1}\right) = a + b{\cdot}d \quad for\ d < c, \tag{1}$$

$$Grain\ weight\ \left(mg\ grain^{-1}\right) = a + b \cdot c \quad for\ d \geq c, \tag{2}$$

where d is the thermal time after silking (°C d^{-1}), a is the y-intercept (mg grain^{-1}), b is the rate of grain-filling (mg grain^{-1} °C d^{-1}), and c is the duration of the period until constant grain weight (°C d^{-1}). The R6 date of a plot was estimated, therefore, when 50% of the sampled plants reached constant grain weight. Thermal time for R6 and other samplings was calculated from the time of silking using a beta-function relationship between the rate of development and hourly temperature (Zhou and Wang, 2018). This method assumes that the developmental rate of the crop is maximal at an optimal temperature (Topt = 33 °C) and is zero at temperatures below a base (Tb = 8 °C) and above the upper temperatures (Tu = 40 °C).

Table 1
Agronomic description and chemical characteristics for pH, organic matter by loss on ignition (measured for the 0–15 cm soil layer), and inorganic N pool by KCl extraction (nitrate and ammonium, measured for the 0–60 cm soil layer) of the three experimental sites used in the study. Soil parameters were measured at pre-planting. Irrigation was performed to maintain soil moisture above 60% of the soil saturation percentage (two and five times, respectively, for 2017 and 2018).

Experiment	Site	Year	Irrigation	Genotype	N rate (kg ha^{-1})	Planting date	Planting density (plants ha^{-1})	^{15}N labelling stages	pH	Organic matter (mg kg^{-1})	$N0_3$–N (mg kg^{-1})	NH_4–N (mg kg^{-1})
1	Ashland Bottoms, KS	2017	Rainfed	3394 - P1197	0–137	May 5, 2017	61,000	R1 – R4	6.1	16	2.4	5.0
2	Ashland Bottoms, KS	2017	Irrigated	3394 - P1197	0–218	May 5, 2017	76,000	R1 – R4	6.1	13	3.2	6.1
3	Ashland Bottoms, KS	2018	Irrigated	3394 - P1197	0–218	April 24, 2018	76,000	R1 – R2 – R5	6.3	15	4.4	3.2

2.2. Isotopic labelled fertilizer application and calculation of ^{15}N plant traits

Stable isotope ^{15}N abundance was utilized as a tracer to determine ^{15}N allocation within plant organs during reproductive stages following the maize phenological scale of Ritchie et al. (1997). The ^{15}N-labelling technique was used at silking (R1) and milk stage (R3) in 2017, and at R1, blister stage (R2), and dough stage (R4) in 2018. For each of these evaluations, microplots containing five consecutive plants in a row were established within each experimental unit. Labelled fertilizer $Ca(NO_3)_2$ (10.15% ^{15}N) at 1 g per plant (equivalent to 6.1–7.6 g m^{-2} depending plant density) was applied with plastic syringes on both sides of the plants after diluting in 30 ml of water. Fertilizer was injected using the methodology employed in de Oliveira Silva et al. (2017). Briefly, holes of 15 cm soil-depth were made on both sides of each plant in the microplot, at a 15 cm distance perpendicular to the row and in a 45° angle. Using 30 ml plastic syringes, labelled fertilizer was injected to holes and, immediately after, 0.5 l of water was applied using PVC pipes (0.6 diameter and 30 cm length) placed on top of each hole. Five days after the ^{15}N application, the three center plants from each microplot were harvested. Additionally, non-enriched plants were sampled to determine the background ^{15}N abundance in the fertilized and unfertilized soils, in order to account for possible variations in the standard values of natural ^{15}N abundance (Cabrera and Kissel, 1989; Högberg, 1997). Plants were separated into leaves (leaf blades), stem (stems + leaf sheaths + tassels), ear (husks + cobs), and grain fractions; after that, samples were dried at 65 °C until constant weight, and then ground through 0.10 mm sieve for laboratory analyses. Elemental abundance of N and C, and ^{15}N abundance, were determined using an elemental analyzer (PyroCube – Elementar Americas) coupled to an isotope ratio mass spectrometer (visION, Elementar Americas, Ronkonkoma, NY, US) at the Stable Isotope Mass Spectrometry Laboratory at Kansas State University.

For each plant fraction, the atom percentage excess [$At\%\ (^{15}N)Excess$] was calculated using the following equation:

$$At\%\ (^{15}N)Excess = At\%\ (^{15}N)_{sample} - At\%\ (^{15}N)_{control}\ , \tag{3}$$

where $At\%\ (^{15}N)_{sample}$ represents the percentage of ^{15}N abundance in the ^{15}N labelled samples, and $At\%\ (^{15}N)_{control}$ corresponds to the percentage of ^{15}N abundance in non-labelled control plants. Total ^{15}N uptake of each fraction and expressed in g m^{-2} was estimated by the following equation:

$$^{15}N\ uptake_{fraction} = N\ uptake_{fraction} \times \left(\frac{At\%\ (^{15}N)Excess_{fraction}}{100}\right), \tag{4}$$

where $N\ uptake_{fraction}$ is the dry biomass multiplied by N concentration and expressed in g m^{-2}. The relative ^{15}N allocation proportion of each fraction was obtained as follows:

$$RA^{15}N = \frac{^{15}N\ uptake_{fraction}}{^{15}N\ uptake_{total}}\ , \tag{5}$$

where $^{15}N\ uptake_{total} = \sum {}^{15}N\ uptake_{fraction\ =\ stem,\ leaves,\ cob-husks,\ grain}$. Lastly, plant C accumulation was calculated as the dry biomass multiplied by C concentration and expressed in g m^{-2}.

2.3. Statistical analyses and calculations

Bayesian generalized additive mixed models (GAMMs) were fitted to the data using R program (version 3.6.1) in RStudio interface (RStudio Team, 2016) with programming language Stan via *brms* package (Bürkner, 2017, 2018). GAMMs are widely used in biological sciences to estimate functional relationships between the explanatory variables and the response using smooth curves (Pykälä et al., 2005; e.g. Yee and Mackenzie, 2002). In this study, we utilized a Bayesian approach via Markov chain Monte Carlo (MCMC) sampling for inference in a mixed model with varying coefficients for genotype and N treatment, random effects to recognize the experimental structure of the data, while including a generalized additive effect for the thermal time after silking.

Relative ^{15}N allocations were modeled using a vector of y_c response variables following a Dirichlet distribution. The Dirichlet distribution is an extension of the beta distribution for C categories with y_c elements between 0 and 1, and for which the sum of all is equal to the unity (Douma and Weedon, 2019). Using a Dirichlet distribution is appropriate here to recognize that the response variable is a vector of inter-dependent proportional values (aggregated observations of four plant fractions). The implemented model was then:

$$y_{ijkl,\ c} \sim Dirichlet(\mu_{ijkl,c},\ \varphi)\ , \tag{6}$$

For each ith N treatment, jth genotype, kth site, lth whole plot within site, and cth plant fraction combination. The expected value for the relative ^{15}N allocation $\mu_{ijkl,\ c}$ is, therefore, between 0 and 1 and subject to the constraint $\sum_{c=1}^{n} \mu_{ijkl,\ c} = 1$ (Douma and Weedon, 2019). In addition, φ is a positive precision parameter, and the link between μ and n is a multinomial logit function $\left[\mu_{ijkl,c} = \frac{\exp(n_{ijkl,c})}{\sum_{d=1}^{m}\exp(n_{ijkl,d})}\right]$ (Bürkner, 2018). For other positive continuous quantities modeled, such as the plant-fraction N and C accumulation, distribution of the response variables was defined as:

$$y_{ijkl} \sim N(\mu_{ijkl},\ \sigma^2)\ , \tag{7}$$

with a log link function $[\mu_{ijkl} = \exp(n_{ijkl})]$. The linear predictor ($n_{ijkl}$) for all models was defined as:

$$n_{ijkl} = n + \alpha_i + \beta_j + \gamma_{ij} + \omega_{ij}(t) + b_k + c_{l(k)j} \tag{8}$$

where α_i and β_j are differential effects of the ith N treatment and jth genotype; γ_{ij} the interaction term between them; b_k is the site-year

random effect for each *k*th site; and $c_{l(k)j}$ is the random effect of the *l*th whole plot within *k*th site and by *j*th genotype. Due to the absence of a rainfed trial in 2018, and the relatively wet growing season in 2017 to explore variability between conditions, the site-year effect was modeled as a random-effect variable allowing to perform a combined analysis among all sites. To describe the nonlinear response patterns of variables expressed in thermal time progress basis, a cubic regression spline $\omega_{ij}(t)$ in the range of time after silking t was included in the model, which depends on the level of *i*th N treatment and *j*th genotype.

Due to the lack of previous information on the likely values of model parameters, non-informative priors were specified for all parameters. Sampling convergence was assessed by visual inspection of density and trace plots, and the use of Gelman-Rubin diagnostics (Gelman and Rubin, 1992). Posterior predictive checks are reported in Supplementary (Fig. S1-S2-S3). Inference was based on 4000 iterations of Markov Chain Monte Carlo (MCMC) algorithm and 4 chains, with a warmup period of 2000 draws for calibration of the MCMC. The implementation of this Bayesian modeling approach enabled the assessment of the expected value of the predicted dynamics while determining a probabilistic component by means of their posterior distribution of samples (Ellison, 2004). The advantage of the implemented Bayesian method over traditional approaches is linked to its flexibility to fit such a complex dataset, offering more options on dealing with uncertainties, and providing posterior density functions which can easily be used for inference at any given set of probability thresholds. Here, we assessed differences between genotypes by evaluating whether the two-sided 95% or 85% credible intervals (for significant or moderate evidence, respectively) of the posterior distribution for the pairwise differences included zero or not.

2.4. Framework to investigate post-silking N dynamics and grain N sources

Using the fitted Bayesian models, and based on the plant N traits introduced in previous section, the internal plant N distribution could be explained in a two-way flux framework. At a given time, N is absorbed and distributed across all stover and grain fractions (exogenous-N). Simultaneously, a fraction of N stored in these organs is remobilized and transported to the developing tissues (endogenous-N). This two-way flux model considers that grains are then sinks of (1) exogenous-N absorbed and directly allocated to grains and (2) endogenous-N translocated from stover, which derives from pre- and post-silking N initially allocated to stems, leaves, and cob-husks.

First, let $N_{fraction}(t)$ be the N content in a fraction at a time t in thermal time after silking, then the net N accumulation rate (i.e. the balance between inward and outward fluxes per unit of time) could be expressed as the first derivative of $N_{fraction}$ with respect to time:

$$\frac{dN_{fraction}}{dt} = \lim_{h\to 0} \frac{N_{fraction}(t+h) - N_{fraction}(t)}{h}, \tag{9}$$

where,

$$N_{fraction}(t) = \%N_{fraction}(t) \times W_{fraction}(t), \tag{10}$$

$\%N_{fraction}$ is the N concentration in that fraction expressed in g 100 g^{-1}, $W_{fraction}$ is the dry weight in g m^{-2}, and $h = \Delta t$ value approaching zero.

Based on equation (9), plant *N uptake rate* at a given time could be estimated using the first derivative of the plant N accumulation,

$$\frac{dN_{plant}}{dt} = \lim_{h\to 0} \frac{N_{plant}(t+h) - N_{plant}(t)}{h}. \tag{11}$$

Considering this two-way flux framework for post-silking dynamics, N derived from uptake (exogenous-N) is allocated to every tissue of the plant at a ratio defined by its $RA^{15}N$ (equation (5)). Therefore, the exogenous-N accumulation rate of a specific fraction at any given time t could be expressed as:

$$\frac{dN^{exo}{}_{fraction}}{dt} = \frac{dN_{plant}}{dt} \times RA^{15}N\,(t), \tag{12}$$

where,

$$RA^{15}N\,(t) = \left[{}^{15}N_{fraction}(t) \,/\, {}^{15}N_{plant}(t)\right]. \tag{13}$$

From there, the endogenous-N rate, which represents the N mobilized to/from each organ, was calculated as the difference between the net N accumulation and the inward flux of exogenous-N rates for that fraction:

$$\frac{dN^{endo}_{fraction}}{dt} = \frac{dN_{fraction}}{dt} - \frac{dN^{endo}_{fraction}}{dt}. \tag{14}$$

The integration of the abovementioned temporal dynamics over the post-silking period (i.e. from $t_{silking} = 0$ to $t_{maturity}$ = *thermal time at R6*) represents the cumulative balance of net N accumulation (15), exogenous-N (16), and endogenous-N (17) on each fraction:

$$\int_{t_{silking}}^{t_{maturity}} \frac{dN_{fraction}}{dt} = N_{fraction}\left(t_{maturity}\right) - N_{fraction}\left(t_{silking}\right), \tag{15}$$

$$\int_{t_{silking}}^{t_{maturity}} \frac{dN^{exo}{}_{fraction}}{dt} = N^{exo}{}_{fraction}\left(t_{maturity}\right) - N^{exo}{}_{fraction}\left(t_{silking}\right), \tag{16}$$

where for post-silking dynamics $N^{exo}{}_{fraction}(t_{silking})$ is the initial state set to zero, and,

$$\int_{t_{silking}}^{t_{maturity}} \frac{dN^{endo}_{fraction}}{dt} = \int_{t_{silking}}^{t_{maturity}} \frac{dN_{fraction}}{dt} - \int_{t_{silking}}^{t_{maturity}} \frac{dN^{exo}_{fraction}}{dt}. \tag{17}$$

3. Results

3.1. Genotypic differences in dry biomass, N uptake, grain yield, and N utilization efficiency

Genotypic variation in dry biomass and N uptake was observed across experiments (Table 2). The P1197 hybrid showed greater grain dry biomass at maturity relative to 3394 under both N conditions. The latter was related also to a higher grain N accumulation at maturity for P1197 compared to 3394, although differences were not significant under zero N. Variations in the stover dry biomass at maturity were mainly related to differences in leaf dry matter between genotypes, which were particularly significant under zero N (138 versus 192 g m^{-2}, for 3394 and P1197 respectively). In addition, stem and cob-husks dry biomass showed little or no variation between genotypes. Similar results of little or no discrepancies between genotypes were obtained for N uptake at maturity in stem, leaf, and cob-husks fractions. Lastly, no genotypic differences in dry matter and N uptake at silking was observed across experiments for these two hybrids.

Grain yield increases in P1197 were primarily driven by enhancement of grain number rather than grain weight. A significant increment on kernel number was identified in P1197 under all N conditions (Table 2). No changes in kernel weight were detected between genotypes, suggesting a less important contribution of this yield component into yield increments. Moreover, to analyze whether genotypes differed in their N conversion efficiency into grain yield, N utilization efficiency was calculated as the ratio of grain dry matter to total N uptake. Overall, P1197 displayed an increased N utilization efficiency than 3394 only under full N, while no differences were observed under zero N. Together, the abovementioned results evidence that genotypic differences in grain yield and N utilization efficiency were more evident under full N, reflecting the better ability of P1197 to respond to N supply.

Table 2
Stem, leaf, cob-husk, and grain dry matter and N uptake at physiological maturity, total dry matter and N uptake at silking, kernel number, kernel weight, and N utilization efficiency (calculated as the ratio of grain yield to total N in aboveground shoot tissue) for 3394 and P1197 hybrids under Zero and Full N conditions during 2017 and 2018. Estimates represent the median of the posterior distributions, and values within square-brackets their 95% credible intervals (CI). Pairwise comparisons were performed between genotypes within N condition.

N level	Genotype	Dry matter at maturity (g m^{-2})				N uptake at maturity (g m^{-2})				Total dry matter at silking (g m^{-2})	Total N uptake at silking (g m^{-2})	Kernel number (kernels m^{-2})	Kernel weight (mg)	N utilization efficiency (grain yield/N uptake)
		Stem	Leaf	Cob-husk	Grain	Stem	Leaf	Cob-husk	Grain					
Zero N	3394	353 [285,424]	138 B [96,185]	167 [96,245]	470 b [294,631]	1.9 [1.2,2.7]	1.2 [0.1,2.5]	1.2 [0.5,2.0]	5.2 [3.8,6.6]	796 [640,956]	6.7 [4.0,9.6]	2311 B [1734,2903]	219 [196,242]	50 [30,76]
	P1197	395 [322,473]	192 A [142,252]	165 [93,249]	589 a [370,761]	2.3 [1.5,3.1]	1.7 [0.4,3.0]	1.4 [0.7,2.2]	6.1 [4.6,7.5]	726 [583,874]	6.1 [3.5,8.8]	3121 A [2530,3723]	212 [188,236]	52 [31,74]
Full N	3394	505 [411,619]	210 [179,246]	244 [183,308]	918 B [675,1084]	4.0 a [3.2,5.1]	2.5 [1.3,4.2]	1.7 [0.9,2.4]	12.1 B [10.9,13.2]	922 [793,1086]	14.7 [12.2,17.2]	3613 B [3148,4088]	276 [259,294]	45 b [31,56]
	P1197	479 [391,584]	231 [199,267]	249 [190,313]	1113 A [833,1292]	3.3 b [2.5,4.3]	3.0 [1.8,4.6]	2.1 [1.3,2.8]	13.6 A [12.6,14.6]	894 [765,1057]	13.7 [11.3,16.2]	4262 A [3808,4732]	283 [266,300]	51 a [36,62]

Different capital letters indicate significant evidence for differences (95% CI of the differences did not include zero).
Different lower case letters indicate moderate evidence for differences (85% CI of the differences did not include zero).

3.2. Exogenous-N uptake was higher in P1197 compared to 3394 under zero and full N

The proportion of ^{15}N allocated to each organ during post-silking was modeled through Bayesian estimation, outlining the internal balance of N across sink tissues (posterior predictive distributions for all four treatment combinations in Fig. 1). Before the initiation of linear grain-filling (0–200 °C d^{-1}), cob-husks tissues were the principal sinks for current N absorbed (on average, 0.34 [0.18, 0.51] g g^{-1} in 3394 and 0.32 [0.16, 0.49] g g^{-1} in P1197; values in brackets define the 95% credible interval, hereafter). Expected allocation to stem + leaves consistently accounted for more than 0.5 g g^{-1} of the N absorbed, but was particularly high under full N supply (0.64 [0.53, 0.76] g g^{-1} in 3394 and 0.62 [0.51, 0.75] g g^{-1} in P1197). As linear-filling progressed, grains emerged as the main sink for N to the detriment of stover provision. Allocation of N absorbed close to physiological maturity (600 °C d^{-1} and beyond) was predominantly to the grains (on average, 0.58 [0.40, 0.74] g g^{-1} in 3394 and 0.57 [0.36, 0.75] g g^{-1} in P1197). At this point, P1197 exposed a marginally greater N distribution to leaves relative to 3394 (respectively for each genotype, 0.18 and 0.10 g g^{-1} for zero N, and 0.22 and 0.17 g g^{-1} for full N). Although the considerable variability observed in the posterior samples, P1197 exhibited greater N allocation to leaves during late grain-filling in 84% (zero-N) and 74% (full-N) of draws obtained, relative to 3394.

The internal N distribution integrated over the post-silking period was assessed in terms of the exogenous- and endogenous-N balances across fractions (Fig. 2). When no N was applied, P1197 exhibited greater exogenous-N accumulated in all organs relative to 3394 (Fig. 2A–D). Under full N, greater exogenous-N was accumulated in P1197 versus 3394 genotype, particularly in leaves and cob-husks fractions. Exogenous-N to the photosynthetic tissues (i.e. green leaves) was 0.8 [0.6, 0.9] g m^{-2} higher in P1197 compared with 3394 (Fig. 2C); for cob-husks, the expected increment was of 0.5 [0.3, 0.7] g m^{-2} (Fig. 2D). Moderate evidence for an increase in exogenous-N to grains in P1997 versus 3394 was found under full N, with an increment around 0.2 [0.1, 0.4] g m^{-2} (Fig. 2A).

3.3. Endogenous-N remobilization was greater in P1197 under full-N condition

Hybrid 3394 accumulated 2.8 [0.1, 5.6] and 5.7 [3.2, 8.1] g m^{-2} of plant N during post-silking (under zero- and full-N, respectively), while P1197 accumulated 5.4 [2.6, 8.1] and 8.2 [6.0, 10.3] g m^{-2}. This enhanced post-silking N uptake in P1197 was well reflected in the grains (Fig. 2I) and, to a lower extent, in the stover net accumulation (Fig. 2J, K, and L). At high N supply, the improved grain N accumulation was predominantly a consequence of more N mobilized from stover tissues (Fig. 2E). Our results indicate that leaves were the primary sources of endogenous-N for the grains, contributing on average 3.0 [1.6, 4.3] g m^{-2} under zero-N and 6.2 [4.9, 7.6] g m^{-2} under full-N (Fig. 2G). P1197 genotype evidenced elevated endogenous-N mobilization only from leaf tissues under full N, although not significant, with a slight increment of 0.79 [0.77, 0.82] g m^{-2} for P1197 under full N (i.e. relative to 3394). Discrepancies in endogenous-N between genotypes were negligible for stem and cob-husks fractions (Fig. 2F and H). This suggests that, at high N availability, the additional exogenous-N accumulated in leaves in P1197 allowed for a larger amount of extractable N mobilized to grains. In contrast, under low N treatment, the increase in exogenous-N to leaves (and for stem and cob-husks) translated to little improvement in endogenous-N. Such patterns suggest dissimilar effects of N fertilization on post-silking N allocation and translocation dynamics for these two maize genotypes.

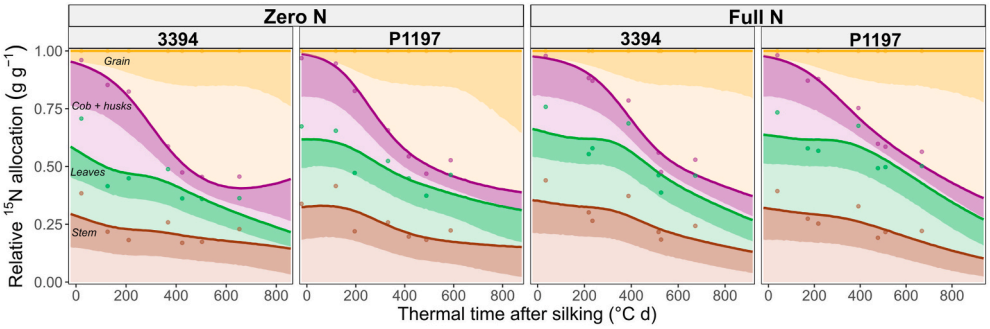

Fig. 1. Relative allocation of ^{15}N ($RA^{15}N$) across plant organs throughout the post-silking period, across two maize hybrids (3394 and P1197) and two N fertilization levels (zero and full N). Solid lines represent medians from samples of the posterior predictive distribution, their corresponding shaded areas represent the 2.5% quantile (i.e. representing half of the 95% credible interval), and symbols show the mean of three replications for each plant fraction × sampling × site.

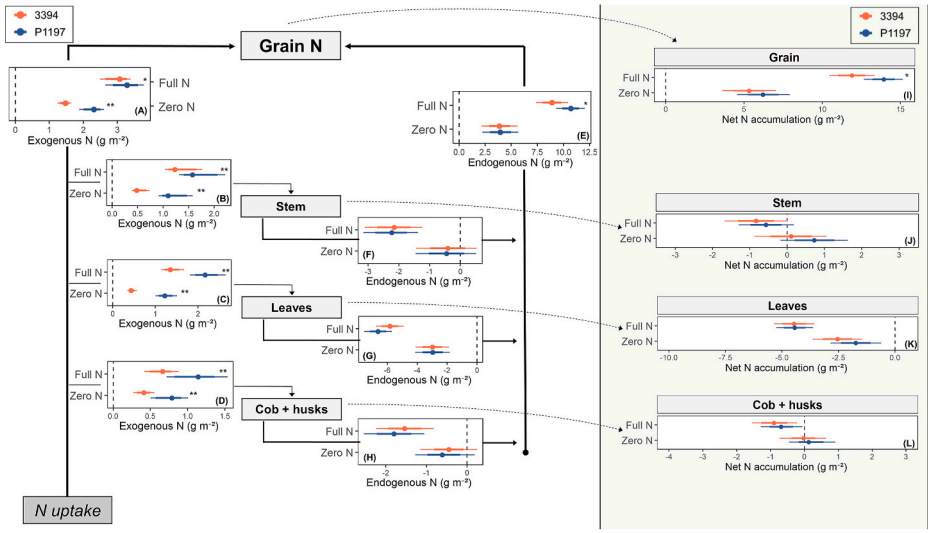

Fig. 2. Summary of posterior predictive distributions for post-silking N allocations in leaves, stem, cob-husks, and grain fractions for two maize hybrids (3394, orange symbols; and P1197, blue symbols) under two N fertilization levels (zero and full N), expressed in g m^{-2} of plot area. Points represent the median of the posterior distributions and whiskers their 95% credible intervals. One or two asterisks indicate moderate or significant evidence for differences (85 or 95% CI of the differences did not include zero, respectively). Values on the left side of the zero-line (dashed line) indicates an export of N from the organ, while to the right, an import of N. Exogenous-N (A, B, C, and D) represents the amount of N absorbed from soil and directly allocated to each organ. Endogenous-N (E, F, G, and H) represents the N translocated from/to other tissues. Net N accumulation (I, J, K and L) represents the difference between N content at R1 and R6. All values represent the cumulative balance over the R1-R6 period (~46 days). Seasonal posterior predictive estimates expressed in thermal time after silking are depicted in Supplementary Fig. S4. (For interpretation of the references to colour in this figure legend, the reader is referred to the Web version of this article.)

3.4. *Exogenous-N allocation to leaves and C accumulation were increased in P1197*

Exogenous-N allocation was further analyzed in proportional terms (over the total N accumulated) to account for the differences in biomass and N uptake between genotypes and fertilization levels. The summary of posterior distributions was depicted against the posteriors for post-silking C accumulation (Fig. 3), reflecting how variations in the within-plant N demand was related to crop growth and C assimilation. Results show that hybrid P1197 showed a greater proportion of N allocated to leaves during this period relative to the older genotype (comparatively for 3394 and P1197, 0.16 and 0.23 g g^{-1} [zero-N] and 0.22 and 0.27 g g^{-1} [full-N]). In contrast, 3394 exhibited proportionally higher allocation towards the grains of the N derived from post-silking uptake (0.51 and 0.41 g g^{-1} [zero-N] and 0.47 and 0.39 g g^{-1} [full-N], respectively for 3394 and P1197). Allocation to stem and cob-

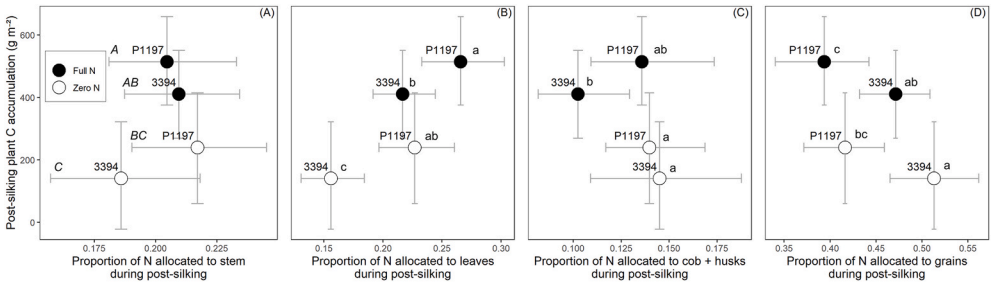

Fig. 3. Summary of the posterior distributions for post-silking plant C accumulation (*y-axis*) and the proportion of exogenous-N (*x-axis*) allocated to (A) stem, (B) leaves, (C) cob-husks, and (D) grains during the post-silking period. Means and credible intervals are depicted for two maize hybrids (3394 and P1197) under two N fertilization levels (zero and full N – open and closed symbols, respectively). Different lower case letters indicate significance differences in the proportion of N allocation (*x-variable*) (α = 0.05). In (A), different capital letters indicate significance differences in post-silking plant C accumulation (*y-variable*).

husks varied little between genotypes, with expected magnitudes of 0.20 [0.18, 0.23] g g^{-1} and 0.13 [0.10, 0.16] g g^{-1} averaged across N levels (respectively for both fractions). Collectively, these outcomes demonstrate that, per unit of N absorbed, P1197 had an improved partitioning to the photosynthetic organs. In 84% of posterior predictive samples, this was related to a better C assimilation of the crop, with an expected C difference between genotypes of 99 g m^{-2} (zero N) and of 103 g m^{-2} (full N).

3.5. Differences in grain N accumulation between genotypes were largely driven by the sink size

As shown in Fig. 2I, expected grain N accumulation at maturity was 5.3 and 6.2 g m^{-2} under zero N (respectively for 3394 and P1197), and increased to 11.9 and 13.9 g m^{-2} under full N treatment. Grain N sources were assessed using the posterior samples for the N derived from exogenous-N (i.e. direct allocation from post-silking uptake) and endogenous-N mobilized from leaves, stem, and cob-husks (i.e. originated from pre- or post-silking N allocated to the stover) (Fig. 4A). Overall, genotypic differences in grain N sources at both N supply conditions were negligible and showed a considerable level of uncertainty (reflected by their 95% credible intervals). Regardless of the genotype and N condition, leaves were the main N sources for grain-filling, contributing with 0.47 [0.33, 0.62] g per g of N in the grains at maturity. Particularly under full-N, stem and cob-husks had a relatively important contribution with expected values of 0.16 [0.09, 0.23] g g^{-1} (stems) and 0.12 [0.06, 0.18] g g^{-1} (cob-husks). In addition, the expected proportion derived from exogenous-N was around 0.28 [0.19, 0.47] g g^{-1} (averaged for both N conditions).

Given the observed variations in grain N sources (Fig. 4A), the relationship between grain weight and N content (at a per kernel basis) was re-explored in terms of exogenous- and endogenous-N quantities (Fig. 4B). The slope between exogenous-N accumulation and dry weight increase per grain varied little between genotypes and N supply levels from 3.0 to 3.8 mg N g^{-1}. Thus, the improvement in exogenous-N allocated to grains in P1197 was essentially a consequence of the sink size (grain number and weight). Under zero-N, average grain number was 2309 and 3125 grains m^{-2} (3394 and P1197, respectively) and grain weight was 219 and 211 mg. On a similar trend under full-N, grain number averaged 3611 and 4259 grains m^{-2} (3394 and P1197, respectively) and grain weight 276 and 283 mg.

4. Discussion

A key scientific pursuit with clear societal and ecological benefits has been the identification of morphological and physiological traits associated with a better N utilization in crops (Hirel et al., 2007). Conceptually, the efficiency in which maize plants use N for seed production has been traditionally associated with manipulations related to N absorption and the N conversion ratio in the reproductive organs (Moll et al., 1982). The ^{15}N multi-stage labelling and posterior two-way N fluxes model developed are useful to quantify the complexity for a larger set of genotypes and a broader range of environmental conditions. Parameterization of the internal N allocation and cycling within plant crop models may improve the understanding of the critical components associated in the N pathway and the identification of future targets of breeding manipulations to enhance N utilization efficiency.

4.1. Coordination between exogenous- and endogenous-N dynamics with N use efficiency

Improvements in exogenous-N absorption in P1197 relative to 3394 were magnified under high-N fertilization. Under these conditions, nitrate and ammonium absorption are expected to occur at a rate closely determined by the plant growth process (Cooper and Clarkson, 1989; Lee et al., 1992). Indeed, greater N uptake in P1197 was accompanied by increases in biomass accumulation (Fernandez et al., 2021). This is in line with a number of studies confirming the association between improvements in N uptake and plant growth in newer hybrids, in particular during the post-silking period (Chen et al., 2016; Ciampitti and Vyn, 2012; Fernandez et al., 2020; Mueller and Vyn, 2016; Tollenaar and Lee, 2006). Considering kernels are the main growing sinks during this period, the increased grain set in P1197 appears to be the main driver for the greater post-silking growth, which subsequently led to increased root N absorption. Even more, the demand rate per kernel of exogenous-N remained stable, even under N-deficiency where other morpho-physiological root traits (e.g. root growth and elongation) are recognized as additional determinants of plant N uptake (Liu et al., 2009; Presterl et al., 2002; Wang et al., 2005). This is in line with studies demonstrating the strong relationship between N uptake and grain development (Ciampitti and Vyn, 2011; Coque and Gallais, 2007; Fageria and Baligar, 2005; Worku et al., 2007). Most importantly, these results highlight the demand-driven regulation exercised by grains over reproductive N uptake in maize plants.

The N framework used here demonstrates that the improvement in exogenous-N uptake was induced by a greater sink size in P1197, but also by an enhanced circulation of post-silking N through the leaves. The greater post-silking N assimilated in P1197 translated to more N allocated to the leaves rather than to the grains. Increasing the proportional N allocation to leaves has been identified as a plausible mechanism for N-efficient plants in other plant species (Laungani and Knops, 2009; Perchlik and Tegeder, 2018). In the present study, the increased amount of N allocated to leaves was re-translocated (as endogenous-N) to the grains as they developed, especially under high N treatment. This

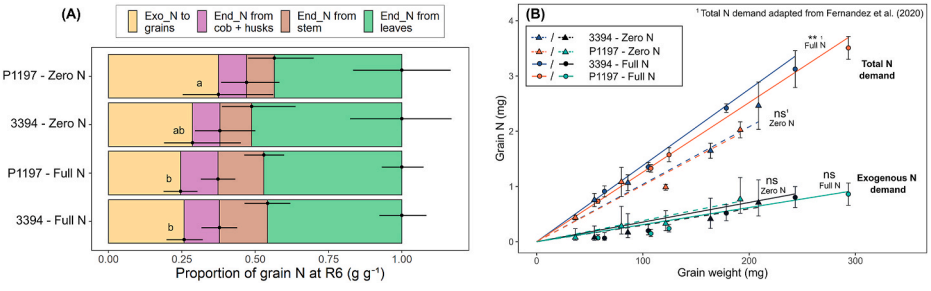

Fig. 4. (A) Sources of grain N at maturity for two maize hybrids (3394 and P1197) under two N fertilization levels (zero and full N - ZN and FN, respectively). The four sources considered are: 1) exogenous-N to grains, which denotes N absorbed and directly allocated to grains during post-silking, and 2–4) Endogenous-N from leaves, stem, and cob-husks, which represents the N translocated respectively from each organ to grains (originated from pre-silking N or post-silking N allocated to the stover). Bars and solid points represent the median from samples of the posterior predictive distribution, and horizontal lines to the right of each bar denotes their corresponding 95% credible interval. (B) Relationship between grain N content and grain weight, throughout the grain filling period, for 3394 and P1197 under zero and full N treatments. Asterisks indicate significant differences between genotypes ($\alpha = 0.05$). Solid line represents the total grain N content for each treatment. Values and differences between genotypes derived from findings in a companion study to this investigation (Fernandez et al., 2021). Dashed lines denote the posterior expectations of exogenous grain N content calculated in the present study. Differences in the exogenous N demand per grain between genotypes were determined by evaluating whether the 95% credible intervals of the pairwise differences (i.e. from the samples produced by the MCMC algorithm) included zero or not.

pattern explains why most of the N imported to the grain at maturity was originated from the leaves/stem N pool and recognizes N mobilization as a key trait in N-efficient genotypes (Chen and Mi, 2018; Masclaux-Daubresse et al., 2010; Tian et al., 2015). Despite the improvements in N uptake capacity, the P1197 hybrid also had an enhanced internal utilization of N for grain production. This was achieved by lowering the grain N requirements which predominantly alleviated the demand for endogenous-N per grain. This strategy allowed a more efficient utilization of the endogenous-N pool to sustain optimal growth in a greater number of grains in this genotype, at the expense of their nutritional value. These findings underscore the necessity to consider the internal N efficiency in crops by considering both exogenous- and endogenous-N as sources for the grain N requirement (Schiltz et al., 2005).

4.2. Carbon fixation as affected by adjustments in leaf N allocation and mobilization

A consistent increase in the proportion of exogenous-N allocated to leaves was observed in the modern hybrid P1197. Regardless of whether N uptake was increased or not, P1197 showed an improved mobilization of new N absorbed through the photosynthetic organs linked to an increase in post-silking C gain. The increment in post-silking C fixation with the greater leaf N allocation raised up the question if the N allocation to leaf has been modified. Leaf N can be categorized as N associated with photosynthetic enzymes and thylakoid N, and the soluble- and insoluble-N pool constituents of cell walls, membranes, and other structures (Mu et al., 2016). In *Arabidopsis* mutants with greater leaf N allocation by means of greater biomass but unchanged content per unit leaf area, enhanced C fixation was a consequence of also an improved investment of N into the synthesis of the photosynthetic components (Perchlik and Tegeder, 2018). Studies in maize (although from a distinct genetic background from the ones used here), showed higher leaf C exchange rates in newer hybrids but only under N-deficiency, by means of improved chlorophyll content and thylakoid electron transport (Echarte et al., 2008). Considering the correlation between leaf N and Rubisco (ribulose-1,5-bisphosphate carboxylase) content, electron transport, and photosynthesis (Dwyer et al., 1995; Eichelmann et al., 2009; Evans, 1989; Meinzer and Zhu, 1998), these outcomes seem to confirm that selection and breeding in maize hybrid development have improved leaf N status under N stress conditions (Boomsma et al., 2009; McCullough et al., 1994). While the specific impacts on the light and dark photosynthetic reactions remains to be determined, the small differences between 3394 and P1197 in green leaf biomass and leaf area under low N (Fernandez et al., 2021) suggest that the enhanced post-silking C fixation may result from adjustments in the leaf N content induced by an optimized exogenous-N supply.

When maize plants were grown under favorable N conditions and the optimum specific leaf N (SLN) content for growth was attained (Sinclair and Horie, 1989), modifications in the chlorophyll and soluble protein content [among which are Rubisco and phosphoenolpyruvate carboxylase (PEPC)] per unit of leaf N hardly affects the net photosynthetic rates (Mu et al., 2016). These findings suggest that the modern hybrid P1197 increased C fixation under high-N by means of a greater total leaf area and a longer retention of green leaves. It therefore seems likely that the enhanced leaf N allocation in P1197 may have been triggered by a greater leaf/shoot ratio (Mueller et al., 2019) and an improved exogenous N supply to preserve the photosynthetic machinery during late grain development (Mu et al., 2018). Furthermore, both genotypes used in this research showed similar SLN content under high N supply (Fernandez et al., 2021). This would imply that the optimized plant N distribution also resulted in a better C fixation efficiency per unit of leaf N, as seen in other species (Atkin et al., 2015; Perchlik and Tegeder, 2018). These results establish that direct selection for yield have indirectly favored N allocation to leaves in modern maize hybrids resulting in an improved post-silking C fixation under high- and low-N availability.

4.3. Implications of N dynamics on yield productivity and N utilization efficiency

As shown in this study, the P1197 genotype achieved greater grain yields and kernel number than the 3394. Breeding progress has increased reproductive resilience and grain set at flowering over time (Messina et al., 2021), establishing a larger reproductive N sink. Here, we provided evidence that the modern genotype could support this larger N demand through two mechanisms, but in a different proportion depending on N availability. First, an increase in post-silking N uptake (i.e. exogenous-N to the grains) under all N conditions. Even more, the greater number of kernels not only increased grain N demand in P1197 but also stimulated post-silking C accumulation and growth. Increased photosynthetic activity may have stimulated N uptake and assimilation in vegetative tissues (Lillo, 2008; Masclaux-Daubresse et al., 2010), reflected here by the ability of P1197 to accommodate more exogenous-N in leaves during post-silking. This led to a greater pool of N to support an increase in N mobilization from the stover (i.e. endogenous-N mostly from leaves), reflecting a second mechanism for the higher N productivity of P1197. The P1197 showed a better remobilization capacity by means of post-silking N allocated to vegetative tissues, which is demonstrated by the fact that both genotypes achieved a similar plant N content at silking. This second mechanism was especially important under high N conditions, where P1197 also evidenced increments in N utilization efficiency relative to 3394. Furthermore, the greater N utilization efficiency was linked to a reduction in grain N concentration. This study establish that the reduction in grain N concentration was linked to the endogenous-N supply to the kernel (i.e. from N-remobilization) rather than to the N derived from post-silking uptake to the grains. It seems improving the N-storage capacity of maize (i.e. either increasing intrinsic N uptake, more N capture per unit of mass or via greater leaf mass) could be key to support further increases in yield with less reduction of the grain N concentration. These findings motivate future research of the significance and alteration of pre-silking N storage and remobilization in maize crops with long-term breeding selection.

Understanding the supply-demand relationship of endogenous-N at a whole-plant scale requires additional consideration on the variation pattern of grain N requirements. In this sense, a lower target of N per grain in P1197 was observed only under high N, which would imply a greater accumulation of starch and therefore lower growth costs per grain (Penning de Vries et al., 1974; Van Iersel, 2003). Although the energetic balance in the plant has not been formally quantified, P1197 showed a superior whole-plant endogenous-N mobilization suggesting altered rates of protein turnover and re-allocation of N (Irving et al., 2010). While recognizing the complexity of reactions involved, it can be argued that further work needs to be conducted evaluating the plant respiratory kinetics across different maize genotypes. Moreover, integrating this information within the two-way flux framework of exogenous-N absorbed and pre-existing endogenous-N may bring an opportunity for models that can account for the protein turnover rates across organs in crops (Loomis and Amthor, 1999).

5. Conclusions

The present study presents a novel approach to study post-silking N allocation and translocation processes for two historical maize genotypes as affected by N availability. By using a dynamic framework of N fluxes considering the external N supply (exogenous-N) and the pre-existing internal N (endogenous-N) in the plant, this research advances our understanding in the adaptive changes in N use with genetic selection over time in these hybrids. Results revealed that the improvement in exogenous-N uptake during post-silking in the newer genotype was induced by both a greater number of grains and an enhanced supply of N to the leaves. Indeed, in proportional terms, hybrid P1197 had a larger partitioning of absorbed N to the photosynthetic organs relative to the older genotype which lead to a better C

assimilation. This greater amount of N into leaves was re-translocated as endogenous-N to the grains and signified a critical N source for final grain N content, especially under high N. These findings establish that direct selection for yield have indirectly favored N allocation to leaves in modern maize hybrids resulting in an improved post-silking C fixation under high- and low-N availability. Moreover, we propose further investigation of the underlying implications on photosynthesis and respiratory system as involved in plant growth. Ultimately, the ^{15}N multi-stage labelling allows for the opportunity to develop meaningful crop models characterizing the internal allocation and recycling of N, and informs selection strategies towards N-efficient genotypes.

Funding

Financial support was provided by Fulbright Program, the Argentine Ministry of Education, Kansas Corn Commission, Corteva Agriscience, and Kansas State University for sponsoring J. A. Fernandez's studies and Dr. I. A. Ciampitti's research program. This is contribution no. 22–127-J from the Kansas Agricultural Experiment Station.

CRediT authorship contribution statement

Javier A. Fernandez: designed and performed research, methodology, data collection and laboratory isotopic analyses, formal analysis, writing – original draft of the manuscript. **Jesse B. Nippert:** conducted the laboratory and isotopic analyses, writing – review & editing. **P.V. Vara Prasad:** writing – review & editing. **Carlos D. Messina:** writing – review & editing. **Ignacio A. Ciampitti:** designed and performed research, methodology, supervision, project administration, funding acquisition, writing – review & editing.

Declaration of competing interest

The authors declare no conflicts of interest.

Acknowledgements

The authors gratefully acknowledge the financial support provided by Fulbright Program, the Argentine Ministry of Education, Kansas Corn Commission, Corteva Agriscience, and Kansas State University for sponsoring J. A. Fernandez's studies and Dr. I. A. Ciampitti's research program.

Appendix A. Supplementary data

Supplementary data to this article can be found online at https://doi.org/10.1016/j.jplph.2021.153577.

References

Arkoun, M., Sarda, X., Jannin, L., Laine, P., Etienne, P., Garcia-Mina, J.-M., Yvin, J.-C., Ourry, A., 2012. Hydroponics versus field lysimeter studies of urea, ammonium and nitrate uptake by oilseed rape(Brassica napus L.). J. Exp. Bot. 63, 5245–5258. https://doi.org/10.1093/jxb/ers183.

Atkin, O.K., Bloomfield, K.J., Reich, P.B., Tjoelker, M.G., Asner, G.P., Bonal, D., Bönisch, G., Bradford, M.G., Cernusak, L.A., Cosio, E.G., Creek, D., Crous, K.Y., Domingues, T.F., Dukes, J.S., Egerton, J.J.G., Evans, J.R., Farquhar, G.D., Fyllas, N. M., Gauthier, P.P.G., Gloor, E., Gimeno, T.E., Griffin, K.L., Guerrieri, R., Heskel, M. A., Huntingford, C., Ishida, F.Y., Kattge, J., Lambers, H., Liddell, M.J., Lloyd, J., Lusk, C.H., Martin, R.E., Maksimov, A.P., Maximov, T.C., Malhi, Y., Medlyn, B.E., Meir, P., Mercado, L.M., Mirotchnick, N., Ng, D., Niinemets, Ü., O'Sullivan, O.S., Phillips, O.L., Poorter, L., Poot, P., Prentice, I.C., Salinas, N., Rowland, L.M., Ryan, M.G., Sitch, S., Slot, M., Smith, N.G., Turnbull, M.H., Vanderwel, M.C., Valladares, F., Veneklaas, E.J., Weerasinghe, L.K., Wirth, C., Wright, I.J., Wythers, K. R., Xiang, J., Xiang, S., Zaragoza-Castells, J., 2015. Global variability in leaf respiration in relation to climate, plant functional types and leaf traits. New Phytol. 206, 614–636. https://doi.org/10.1111/nph.13253.

Avice, J.C., Ourry, A., Lemaire, G., Boucaud, J., 1996. Nitrogen and carbon flows estimated by 15N and 13C pulse-chase labeling during regrowth of Alfalfa. Plant Physiol. 112, 281–290. https://doi.org/10.1104/pp.112.1.281.

Boomsma, C.R., Santini, J.B., Tollenaar, M., Vyn, T.J., 2009. Maize morphophysiological responses to intense crowding and low nitrogen availability: an analysis and review. Agron. J. 101, 1426–1452. https://doi.org/10.2134/agronj2009.0082.

Borrell, A.K., Hammer, G.L., 2000. Nitrogen dynamics and the physiological basis of stay-green in Sorghum. Crop Sci. 40, 1295–1307. https://doi.org/10.2135/cropsci2000.4051295x.

Bürkner, P.C., 2018. Advanced Bayesian multilevel modeling with the R package brms. R J. https://doi.org/10.32614/rj-2018-017.

Bürkner, P.C., 2017. brms: an R package for Bayesian multilevel models using Stan. J. Stat. Software. https://doi.org/10.18637/jss.v080.i01.

Cabrera, M.L., Kissel, D.E., 1989. Review and simplification of calculations in 15N tracer studies. Fert. Res. 20, 11–15.

Chen, K., Camberato, J.J., Tuinstra, M.R., Kumudini, S.V., Tollenaar, M., Vyn, T.J., 2016. Genetic improvement in density and nitrogen stress tolerance traits over 38 years of commercial maize hybrid release. Field Crop. Res. 196, 438–451. https://doi.org/10.1016/j.fcr.2016.07.025.

Chen, K., Kumudini, S.V., Tollenaar, M., Vyn, T.J., 2015. Plant biomass and nitrogen partitioning changes between silking and maturity in newer versus older maize hybrids. Field Crop. Res. 183, 315–328. https://doi.org/10.1016/j.fcr.2015.08.013.

Chen, Y., Mi, G., 2018. Physiological mechanisms underlying post-silking nitrogen use efficiency of high-yielding maize hybrids differing in nitrogen remobilization efficiency. J. Plant Nutr. Soil Sci. 181, 923–931. https://doi.org/10.1002/jpln.201800161.

Ciampitti, I.A., Vyn, T.J., 2012. Physiological perspectives of changes over time in maize yield dependency on nitrogen uptake and associated nitrogen efficiencies: a review. Field Crop. Res. 133, 48–67. https://doi.org/10.1016/j.fcr.2012.03.008.

Ciampitti, I.A., Vyn, T.J., 2011. A comprehensive study of plant density consequences on nitrogen uptake dynamics of maize plants from vegetative to reproductive stages. Field Crop. Res. 121, 2–18. https://doi.org/10.1016/j.fcr.2010.10.009.

Cliquet, J.-B., Deleens, E., Mariotti, A., 1990. C and N mobilization from stalk and leaves during kernel filling by 13C and 15N tracing in Zea mays L. Plant Physiol. 94, 1547–1553. https://doi.org/10.1104/pp.94.4.1547.

Cooper, H.D., Clarkson, D.T., 1989. Cycling of amino-nitrogen and other nutrients between shoots and roots in cereals—a possible mechanism integrating shoot and root in the regulation of nutrient uptake. J. Exp. Bot. 40, 753–762. https://doi.org/10.1093/jxb/40.7.753.

Coque, M., Gallais, A., 2007. Genetic variation for nitrogen remobilization and postsilking nitrogen uptake in maize recombinant inbred lines: heritabilities and correlations among traits. Crop Sci. 47, 1787–1796.

Crawford, T.W., Rendig, V.V., Broadbent, F.E., 1982. Sources, fluxes, and sinks of nitrogen during early reproductive growth of maize (Zea mays L.). Plant Physiol. 70, 1654–1660. https://doi.org/10.1104/pp.70.6.1654.

de Oliveira Silva, A., Camberato, J.J., Coram, T., Filley, T., Vyn, T.J., 2017. Applicability of a "multi-stage pulse labeling" 15N approach to phenotype N dynamics in maize plant components during the growing season. Front. Plant Sci. 8, 1–17. https://doi.org/10.3389/fpls.2017.01360.

DeBruin, J.L., Schussler, J.R., Mo, H., Cooper, M., 2017. Grain yield and nitrogen accumulation in maize hybrids released during 1934 to 2013 in the US Midwest. Crop Sci. 57, 1431–1446. https://doi.org/10.2135/cropsci2016.08.0704.

Douma, J.C., Weedon, J.T., 2019. Analysing continuous proportions in ecology and evolution: a practical introduction to beta and Dirichlet regression. Methods Ecol. Evol. 10, 1412–1430. https://doi.org/10.1111/2041-210X.13234.

Dreccer, M.F., Schapendonk, A.H.C.M., Slafer, G.A., Rabbinge, R., 2000. Comparative response of wheat and oilseed rape to nitrogen supply: absorption and utilisation efficiency of radiation and nitrogen during the reproductive stages determining yield. Plant Soil 220, 189–205. https://doi.org/10.1023/a:1004757124939.

Duvick, D.N., 2005. Genetic progress in yield of United States maize (Zea mays L.). Maydica 50, 193–202.

Dwyer, L.M., Anderson, A.M., Stewart, D.W., Ma, B.L., Tollenaar, M., 1995. Changes in maize hybrid photosynthetic response to leaf nitrogen, from pre-anthesis to grain fill. Agron. J. 87, 1221–1225. https://doi.org/10.2134/agronj1995.00021962008700060031x.

Echarte, L., Rothstein, S., Tollenaar, M., 2008. The response of leaf photosynthesis and dry matter accumulation to nitrogen supply in an older and a newer maize hybrid. Crop Sci. 48, 656–665. https://doi.org/10.2135/cropsci2007.06.0366.

Eichelmann, H., Talts, E., Oja, V., Padu, E., Laisk, A., 2009. Rubisco in planta kcat is regulated in balance with photosynthetic electron transport. J. Exp. Bot. 60, 4077–4088. https://doi.org/10.1093/jxb/erp242.

Ellison, A.M., 2004. Bayesian inference in ecology. Ecol. Lett. 7, 509–520. https://doi.org/10.1111/j.1461-0248.2004.00603.x.

Evans, J.R., 1989. Photosynthesis and nitrogen relationships in leaves of C_3 plants. Oecologia 78, 9–19.

Fageria, N.K., Baligar, V.C., 2005. Enhancing nitrogen use efficiency in crop plants. Adv. Agron. 88, 97–185. https://doi.org/10.1016/S0065-2113(05)88004-6.
Fernandez, J.A., DeBruin, J., Messina, C.D., Ciampitti, I.A., 2020. Late-season nitrogen fertilization on maize yield: a meta-analysis. Field Crop. Res. 247, 107586. https://doi.org/10.1016/j.fcr.2019.107586.
Fernandez, J.A., Messina, C.D., Rotundo, J.L., Ciampitti, I.A., 2021. Integrating nitrogen and water-soluble carbohydrates dynamics in maize: a comparison of hybrids from different decades. Crop Sci. 61, 1360–1373. https://doi.org/10.1002/csc2.20338.
Friedrich, J.W., Schrader, L.E., 1979. N deprivation in maize during grain-filling. II. Remobilization of 15N and 35S and the relationship between N and S accumulation. Agron. J. 71, 466–472. https://doi.org/10.2134/agronj1979.00021962007100030021x.
Gallais, A., Coque, M., Quilléré, I., Prioul, J.L., Hirel, B., 2006. Modelling postsilking nitrogen fluxes in maize (Zea mays) using 15N-labelling field experiments. New Phytol. 172, 696–707. https://doi.org/10.1111/j.1469-8137.2006.01890.x.
Gelman, A., Rubin, D.B., 1992. Inference from iterative simulation using multiple sequences. Stat. Sci. 7, 457–472. https://doi.org/10.1214/ss/1177011136.
Haegele, J.W., Cook, K.A., Nichols, D.M., Below, F.E., 2013. Changes in nitrogen use traits associated with genetic improvement for grain yield of maize hybrids released in different decades. Crop Sci. 53, 1256–1268. https://doi.org/10.2135/cropsci2012.07.0429.
Hirel, B., Le Gouis, J., Ney, B., Gallais, A., 2007. The challenge of improving nitrogen use efficiency in crop plants: towards a more central role for genetic variability and quantitative genetics within integrated approaches. J. Exp. Bot. 58, 2369–2387. https://doi.org/10.1093/jxb/erm097.
Hirose, T., Werger, M.J.A., 1987. Maximizing daily canopy photosynthesis with respect to the leaf nitrogen allocation pattern in the canopy. Oecologia 72, 520–526. https://doi.org/10.1007/BF00378977.
Högberg, P., 1997. Tansley Review No. 95 15N natural abundance in soil–plant systems. New Phytol. 137, 179–203.
Hollinger, D.Y., 1996. Optimality and nitrogen allocation in a tree canopy. Tree Physiol. 16, 627–634. https://doi.org/10.1093/treephys/16.7.627.
Irving, L.J., Suzuki, Y., Ishida, H., Makino, A., 2010. Protein turnover in grass leaves. In: Advances in Botanical Research, pp. 139–182. https://doi.org/10.1016/S0065-2296(10)54004-7.
Kinugasa, T., Sato, T., Oikawa, S., Hirose, T., 2012. Demand and supply of N in seed production of soybean (Glycine max) at different N fertilization levels after flowering. J. Plant Res. 125, 275–281. https://doi.org/10.1007/s10265-011-0439-5.
Knowles, R., Blackburn, T.H. (Eds.), 1993. Nitrogen Isotope Techniques. Academic Press, Inc., San Diego, California, USA.
Kosgey, J.R., Moot, D.J., Fletcher, A.L., McKenzie, B.A., 2013. Dry matter accumulation and post-silking N economy of “stay-green” maize (Zea mays L.) hybrids. Eur. J. Agron. 51, 43–52. https://doi.org/10.1016/j.eja.2013.07.001.
Ladha, J.K., Tirol-Padre, A., Reddy, C.K., Cassman, K.G., Verma, S., Powlson, D.S., Van Kessel, C., De Richter, D.B., Chakraborty, D., Pathak, H., 2016. Global nitrogen budgets in cereals: a 50-year assessment for maize, rice, and wheat production systems. Sci. Rep. 6, 1–9. https://doi.org/10.1038/srep19355.
Lambers, H., Chapin, F.S., Pons, T.L., 2008. Plant physiological ecology. In: Plant Physiological Ecology, second ed. Springer New York, New York, NY. https://doi.org/10.1007/978-0-387-78341-3.
Laungani, R., Knops, J.M.H., 2009. Species-driven changes in nitrogen cycling can provide a mechanism for plant invasions. Proc. Natl. Acad. Sci. U.S.A. 106, 12400–12405. https://doi.org/10.1073/pnas.0900921106.
Lee, R.B., Purves, J.V., Ratcliffe, R.G., Saker, L.R., 1992. Nitrogen assimilation and the control of ammonium and nitrate absorption by maize roots. J. Exp. Bot. 43, 1385–1396. https://doi.org/10.1093/jxb/43.11.1385.
Lehmeier, C.A., Wild, M., Schnyder, H., 2013. Nitrogen stress affects the turnover and size of nitrogen pools supplying leaf growth in a grass. Plant Physiol. 162, 2095–2105. https://doi.org/10.1104/pp.113.219311.
Lillo, C., 2008. Signalling cascades integrating light-enhanced nitrate metabolism. Biochem. J. 415, 11–19. https://doi.org/10.1042/BJ20081115.
Liu, J., Chen, F., Olokhnuud, C., Glass, A.D.M., Tong, Y., Zhang, F., Mi, G., 2009. Root size and nitrogen-uptake activity in two maize (Zea mays) inbred lines differing in nitrogen-use efficiency. J. Plant Nutr. Soil Sci. 172, 230–236. https://doi.org/10.1002/jpln.200800028.
Loomis, R.S., Amthor, J.S., 1999. Yield potential, plant assimilatory capacity, and metabolic efficiencies. Crop Sci. 39, 1584–1596. https://doi.org/10.2135/cropsci1999.3961584x.
Malagoli, P., Laine, P., Rossato, L., Ourry, A., 2005. Dynamics of nitrogen uptake and mobilization in field-grown winter oilseed rape (Brassica napus) from stem extension to harvest. II. An 15N-labelling-based simulation model of N partitioning between vegetative and reproductive tissues. Ann. Bot. 95, 1187–1198. https://doi.org/10.1093/aob/mci131.
Masclaux-Daubresse, C., Daniel-Vedele, F., Dechorgnat, J., Chardon, F., Gaufichon, L., Suzuki, A., 2010. Nitrogen uptake, assimilation and remobilization in plants: challenges for sustainable and productive agriculture. Ann. Bot. 105, 1141–1157. https://doi.org/10.1093/aob/mcq028.
McCullough, D.E., Girardin, P., Mihajlovic, M., Aguilera, A., Tollenaar, M., 1994. Influence of N supply on development and dry matter accumulation of an old and a new maize hybrid. Can. J. Plant Sci. 74, 471–477. https://doi.org/10.4141/cjps94-087.
Meinzer, F.C., Zhu, J., 1998. Nitrogen stress reduces the efficiency of the C4CO2 concentrating system, and therefore quantum yield, in Saccharum (sugarcane) species. J. Exp. Bot. 49, 1227–1234. https://doi.org/10.1093/jxb/49.324.1227.
Messina, C., McDonald, D., Poffenbarger, H., Clark, R., Salinas, A., Fang, Y., Gho, C., Tang, T., Graham, G., Hammer, G.L., Cooper, M., 2021. Reproductive resilience but not root architecture underpins yield improvement under drought in maize. J. Exp. Bot. 72, 5235–5245. https://doi.org/10.1093/jxb/erab231.
Moll, R.H., Kamprath, E.J., Jackson, W.A., 1982. Analysis and interpretation of factors which contribute to efficiency of nitrogen utilization. Agron. J. https://doi.org/10.2134/agronj1982.00021962007400030037x.
Mu, X., Chen, Q., Chen, F., Yuan, L., Mi, G., 2018. Dynamic remobilization of leaf nitrogen components in relation to photosynthetic rate during grain filling in maize. Plant Physiol. Biochem. 129, 27–34. https://doi.org/10.1016/j.plaphy.2018.05.020.
Mu, X., Chen, Q., Chen, F., Yuan, L., Mi, G., 2016. Within-leaf nitrogen allocation in adaptation to low nitrogen supply in maize during grain-filling stage. Front. Plant Sci. 7, 699. https://doi.org/10.3389/fpls.2016.00699.
Mueller, S.M., Messina, C.D., Vyn, T.J., 2019. Simultaneous gains in grain yield and nitrogen efficiency over 70 years of maize genetic improvement. Sci. Rep. 9, 9095. https://doi.org/10.1038/s41598-019-45485-5.
Mueller, S.M., Vyn, T.J., 2016. Maize plant resilience to N stress and post-silking N capacity changes over time: a review. Front. Plant Sci. 7, 1–14. https://doi.org/10.3389/fpls.2016.00053.
Penning de Vries, F.W.T., Brunsting, A.H.M., Van Laar, H.H., 1974. Products, requirements and efficiency of biosynthesis a quantitative approach. J. Theor. Biol. 45, 339–377. https://doi.org/10.1016/0022-5193(74)90119-2.
Perchlik, M., Tegeder, M., 2018. Leaf amino acid supply affects photosynthetic and plant nitrogen use efficiency under nitrogen stress. Plant Physiol. 178, 174–188. https://doi.org/10.1104/pp.18.00597.
Presterl, T., Groh, S., Landbeck, M., Seitz, G., Schmidt, W., Geiger, H.H., 2002. Nitrogen uptake and utilization efficiency of European maize hybrids developed under conditions of low and high nitrogen input. Plant Breed. 121, 480–486. https://doi.org/10.1046/j.1439-0523.2002.00770.x.
Pykälä, J., Luoto, M., Heikkinen, R.K., Kontula, T., 2005. Plant species richness and persistence of rare plants in abandoned semi-natural grasslands in northern Europe. Basic Appl. Ecol. 6, 25–33. https://doi.org/10.1016/j.baae.2004.10.002.
Ritchie, S.W., Hanway, J.J., Benson, G.O., 1997. How a Corn Plant Develops. Spec. Rep. No, vol. 48. Iowa State Univ. Sci. Technol. Coop. Ext. Serv., Ames, IA.
Rossato, L., Lainé, P., Ourry, A., 2001. Nitrogen storage and remobilization in Brassica napus L. during the growth cycle: nitrogen fluxes within the plant and changes in soluble protein patterns. J. Exp. Bot. 52, 1655–1663. https://doi.org/10.1093/jxb/52.361.1655.
RStudio Team, 2016. RStudio. Integrated Development for R. RStudio, Inc., Boston, MA.
Russelle, M.P., Hauck, R.D., Olson, R.A., 1983. Nitrogen accumulation rates of irrigated maize. Agron. J. 75, 593. https://doi.org/10.2134/agronj1983.00021962007500040006x.
Salon, C., Munier-Jolain, N.G., Duc, G.G., Voisin, A.-S., Grandgirard, D., Larmure, A., Emery, R.J.N., Ney, B., 2001. Grain legume seed filling in relation to nitrogen acquisition: a review and prospects with particular reference to pea. Agronomie 21, 539–552. https://doi.org/10.1051/agro:2001143.
Schiltz, S., Munier-Jolain, N., Jeudy, C., Burstin, J., Salon, C., 2005. Dynamics of exogenous nitrogen partitioning and nitrogen remobilization from vegetative organs in pea revealed by 15 N in vivo labeling throughout seed filling. Plant Physiol. 137, 1463–1473. https://doi.org/10.1104/pp.104.056713.
Sinclair, T.R., Horie, T., 1989. Leaf nitrogen, photosynthesis, and crop radiation use efficiency: a review. Crop Sci. 29, 90–98. https://doi.org/10.2135/cropsci1989.0011183X002900010023x.
Sinclair, T.R., Rufty, T.W., 2015. Genetic improvement of water and nitrogen use to increase crop yields: a whole plant physiological perspective. In: Drechsel, P., Heffer, P., Magen, H., Mikkelsen, R., Wichelns, D. (Eds.), Managing Water and Fertilizer for Sustainable Agricultural Intensification. International Fertilizer Industry Association (IFA), Internatio- Nal Water Management Institute (IWMI), International Plant Nutrition Institute (IPNI), and International Potash. Institute (IPI)., Paris, France, pp. 87–108.
Ta, C.T., Weiland, R.T., 1992. Nitrogen partitioning in maize during ear development. Crop Sci. 32, 443–451. https://doi.org/10.2135/cropsci1992.0011183x003200020032x.
Tanemura, R., Kurashima, H., Ohtake, N., Sueyoshi, K., Ohyama, T., 2008. Absorption and translocation of nitrogen in cucumber (Cucumis sativus L.) plants using the 15 N tracer technique. Soil Sci. Plant Nutr. 54, 108–117. https://doi.org/10.1111/j.1747-0765.2007.00213.x.
Tegeder, M., Masclaux-Daubresse, C., 2018. Source and sink mechanisms of nitrogen transport and use. New Phytol. 217, 35–53. https://doi.org/10.1111/nph.14876.
Tian, H., Fu, J., Drijber, R.A., Gao, Y., 2015. Expression patterns of five genes involved in nitrogen metabolism in two winter wheat (Triticum aestivum L.) genotypes with

high and low nitrogen utilization efficiencies. J. Cereal. Sci. 61, 48–54. https://doi.org/10.1016/j.jcs.2014.09.007.
Tollenaar, M., Lee, E.A., 2006. Dissection of physiological processes underlying grain yield in maize by examining genetic improvement and heterosis, 51, pp. 399–408.
Van Iersel, M.W., 2003. Carbon use efficiency depends on growth respiration, maintenance respiration, and relative growth rate. A case study with lettuce. Plant Cell Environ. 26, 1441–1449. https://doi.org/10.1046/j.0016-8025.2003.01067.x.
Vos, J., Van Der Putten, P.E.L., Birch, C.J., 2005. Effect of nitrogen supply on leaf appearance, leaf growth, leaf nitrogen economy and photosynthetic capacity in maize (Zea mays L.). Field Crop. Res. 93, 64–73. https://doi.org/10.1016/j.fcr.2004.09.013.
Wang, Y., Mi, G., Chen, F., Zhang, J., Zhang, F., 2005. Response of root morphology to nitrate supply and its contribution to nitrogen accumulation in maize. J. Plant Nutr. 27, 2189–2202. https://doi.org/10.1081/PLN-200034683.
Weiland, R., Ta, T., 1992. Allocation and retranslocation of 15N by maize (Zea mays L.) hybrids under field conditions of low and high N fertility. Funct. Plant Biol. 19, 77. https://doi.org/10.1071/PP9920077.
Worku, M., Bänziger, M., Erley, G.S.A.m., Friesen, D., Diallo, A.O., Horst, W.J., 2007. Nitrogen uptake and utilization in contrasting nitrogen efficient tropical maize hybrids. Crop Sci. 47, 519–528. https://doi.org/10.2135/cropsci2005.05.0070.
Yang, L., Guo, S., Chen, Q., Chen, F., Yuan, L., Mi, G., 2016. Use of the stable nitrogen isotope to reveal the source-sink regulation of nitrogen uptake and remobilization during grain filling phase in maize. PLoS One 11, 1–16. https://doi.org/10.1371/journal.pone.0162201.
Yee, T.W., Mackenzie, M., 2002. Vector generalized additive models in plant ecology. Ecol. Model. 157, 141–156. https://doi.org/10.1016/S0304-3800(02)00192-8.
Yoneyama, T., Ito, O., Engelaar, W.M.H.G., 2003. Uptake, metabolism and distribution of nitrogen in crop plants traced by enriched and natural 15N: progress over the last 30 years. Phytochemistry Rev. 2, 121–132. https://doi.org/10.1023/B:PHYT.0000004198.95836.ad.
Zhou, G., Wang, Q., 2018. A new nonlinear method for calculating growing degree days. Sci. Rep. 8, 1–14. https://doi.org/10.1038/s41598-018-28392-z.